CHAPTER 6

The "curl side": Complementarity

We return to the model problem of Chapter 2, the magnetostatics version of the "Bath cube" setup. This time, the two mirror symmetries with respect to vertical planes are taken into account (Fig. 6.1): The field b is obviously invariant with respect to both reflections, hence $n \cdot b = 0$ on these planes.[1]

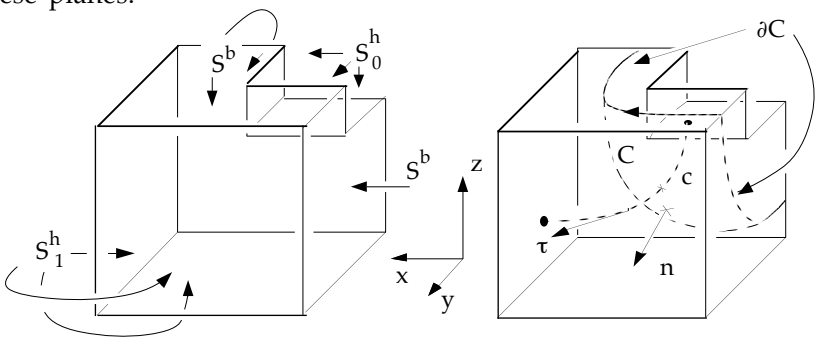

FIGURE 6.1. Notations for solving the Bath-cube magnetostatics problem in a quarter of the cavity. Symmetry planes bear the boundary condition $n \cdot b = 0$, hence contributing to the S^b boundary. The "link" c must go from the upper pole (here, part S^h_0 of the boundary S^h) to the lower pole (part S^h_1 of S^h), whereas the "cut" C should separate the two poles, while having its own boundary ∂C inside S^b. (In the jargon of Fig. 4.6, c and C are "closed mod S^h [resp. mod S^b] and non-bounding".)

Denoting by D the domain thus defined, and by S its boundary, with S^h the "magnetic boundary" and S^b the part of S at the top of the cavity (cf. Fig. 2.6) and in symmetry planes, we must have:

[1]We could reduce further to an eighth, by taking into account the invariance with respect to a 90° rotation around the z-axis. But the symmetry group thus obtained is not Abelian, a feature which considerably complicates the exploitation of symmetry. Cf. Refs. [B1, B2] of Appendix A.

(1) $\text{rot}\, h = 0$ in D, (3) $\text{div}\, b = 0$ in D,

(2) $n \times h = 0$ on S^h (4) $n \cdot b = 0$ on S^b,

(5) $b = \mu h$ in D.

The problem is made well-posed by imposing one of the two conditions

(6) $\int_c \tau \cdot h = I$, (7) $\int_C n \cdot b = F$,

as we saw[2] in 2.4.1. These equations are the same as (2.20)–(2.26), and little changed in the former model due to geometrical symmetry, except for one thing: The flux F in (7) is now the flux through one-quarter of the device, and the computed reluctance will be relative to a quarter as well.

The layout of Eqs. (1–7) underlines a symmetry of another kind, which will be our main concern in this chapter: the symmetry of the magnetostatic equations *with respect to the* b–h *interchange*. This can be made even more patent by setting the problem as follows: We look for *pairs* {F, I} for which problem (1–7) has a solution. By linearity, they all lie on the characteristic line $I = RF$ in the F–I plane, and the problem thus consists in finding R. (This remark, though of moderate interest in the present linear case, is the key to nonlinear generalization [B3].)

6.1 A SYMMETRICAL VARIATIONAL FORMULATION

We shall strive to preserve this symmetry in the search for a variational formulation. The functional point of view continues to prevail: We look for the solution as (first step) an element of some predefined functional space that (second step) can be characterized as the minimizer of some easily interpretable, energy-related quantity.

6.1.1 Spaces of admissible fields

By "the" solution, now, we mean the *pair* {h, b}. What are the eligible fields, a priori? Both h and b will certainly belong to $\mathbb{L}^2(D)$, since magnetic energy is finite. Moreover, $\text{rot}\, h = 0$ and $\text{div}\, b = 0$, and if we had to generalize what we do to cases where a given current density j

[2]The relative arbitrariness in the choice of c and C is reminded (cf. Exers. 2.5, 2.6 and Fig. 4.6). In precise language, integrals (6) and (7) depend on the *homology classes* of c and C, mod S^h and mod S^b, respectively.

exists in the cavity, $\mathrm{rot}\, h \equiv j$ would be square-integrable, since Joule dissipation must remain finite. This points to $\mathbb{L}^2_{\mathrm{rot}}(D)$ as the space in which to look for h. Symmetrically, b will belong to $\mathbb{L}^2_{\mathrm{div}}(D)$.

We can do better, by anticipating a little on the discretization process yet to come. Some a priori constraints on the solution are easy to enforce at the discretized level (those are the "essential" or "Dirichlet-like" conditions mentioned in 2.4.4), and it pays to take them into account from the onset in the definition of admissible fields, since this reduces the scope of the search. Boundary conditions (3) and (4) are of this kind. So let us define (recall we are now using the *weak* grad, rot, div)

$$\mathbb{H} = \{h \in \mathbb{L}^2_{\mathrm{rot}}(D) :\ \mathrm{rot}\, h = 0,\ n \times h = 0 \ \text{ on } S^h\},$$

$$\mathbb{B} = \{b \in \mathbb{L}^2_{\mathrm{div}}(D) :\ \mathrm{div}\, b = 0,\ n \cdot b = 0 \ \text{ on } S^b\}.$$

These are closed subspaces of $\mathbb{L}^2(D)$, after Exer. 5.3. We note that fields of the form $h = \mathrm{grad}\, \varphi$ belong to $\mathbb{H}$ if φ is a potential which assumes constant values on both parts of the magnetic boundary S^h (not necessarily the same constant on each), and we recycle the symbol Φ to denote the space of such potentials:

$$\Phi = \{\varphi \in L^2_{\mathrm{grad}}(D) :\ n \times \mathrm{grad}\, \varphi = 0 \ \text{ on } S^h\}.$$

(It's not exactly the same as the earlier Φ, beware: φ is a constant on S^h_0, but not necessarily the constant 0.) Similarly, on the side of b, let's introduce

$$A = \{a \in \mathbb{L}^2_{\mathrm{rot}}(D) :\ n \cdot \mathrm{rot}\, a = 0 \ \text{ on } S^b\},$$

and remark that fields of the form $b = \mathrm{rot}\, a$, with $a \in A$, belong to $\mathbb{B}$. Moreover, if D is contractible (no loops, no holes[3]) then, by the Poincaré lemma (understood in its extended version of 5.1.4),

$$(8) \qquad \mathbb{H} = \mathrm{grad}\, \Phi, \qquad\qquad \mathbb{B} = \mathrm{rot}\, A,$$

instead of mere inclusions.

Conditions (6) and (7) also can be enforced a priori. Let's define linear functionals $\mathcal{J} : \mathbb{H} \to \mathbb{R}$ and $\mathcal{F} : \mathbb{B} \to \mathbb{R}$ as follows. First, if h and b are smooth, set

$$\mathcal{J}(h) = \int_c \tau \cdot h, \qquad\qquad \mathcal{F}(b) = \int_C n \cdot b,$$

[3]The reader who suspects that (8) may hold in spite of the existence of loops or holes in D, for more complex geometries, is right. Only *relative* loops and holes (mod S^h and S^b) are harmful.

Then, let us prove the following:

Proposition 6.1. *$\mathcal{J}$ and $\mathcal{F}$ have extensions,* continuous *with respect to the metric of* $\mathbb{L}^2(D)$, *to* $\mathbb{H}$ *and* $\mathbb{B}$.

Proof. Let φ^1 be a smooth function assuming the values 0 on S^h_0 and 1 on S^h_1. For $b \in \mathbb{B}$, then, $\int_D b \cdot \text{grad}\, \varphi^1 = \int_S n \cdot b\ \varphi^1 = \int_{S^h_1} n \cdot b = \mathcal{F}(b)$, as we saw with Exer. 2.6, and the map $b \to \int_D b \cdot \text{grad}\, \varphi^1$, which is $\mathbb{L}^2$-continuous, is thus the announced extension. The proof for $\mathcal{J}$ is a bit more involved. (Doing now Exercise 6.6 on p. 187, as preparation, may help.) Pick a smooth vector field a^1 such that $n \cdot \text{rot}\, a^1 = 0$ on S^b and $\int_C n \cdot \text{rot}\, a^1 = 1$. For $h \equiv \text{grad}\, \varphi \in \mathbb{H}$, then, $\int_D h \cdot \text{rot}\, a^1 = -\int_S n \times h \cdot a^1 = -\int_S n \times \text{grad}\, \varphi \cdot a^1 = \int_S n \times a^1 \cdot \text{grad}\, \varphi = -\int_S \text{div}(n \times a^1)\ \varphi = -\int_S n \cdot \text{rot}\, a^1\, \varphi = -\int_{S^h} n \cdot \text{rot}\, a^1\, \varphi = \mathcal{J}(h) \int_C n \cdot \text{rot}\, a^1 = \mathcal{J}(h)$. Again, the continuity of $h \to \int_D h \cdot \text{rot}\, a^1$ proves the point. From now on, we let $\mathcal{J}$ and $\mathcal{F}$ denote the extended continuous functionals. ◊

Remark 6.1. Integrals such as $\mathcal{J}$ and $\mathcal{F}$ stand no chance of being $\mathbb{L}^2(D)$-continuous if one tries to enlarge their domains beyond $\mathbb{H}$ and $\mathbb{B}$. The conditions $\text{rot}\, h = 0$ and $\text{div}\, b = 0$ are necessary. ◊

As a corollary, subspaces

$$\mathbb{H}^I = \{h \in \mathbb{H} : \int_c \tau \cdot h = I\}, \qquad \mathbb{B}^F = \{b \in \mathbb{B} : \int_C n \cdot b = F\},$$

are closed. By (8), we have $\mathbb{H}^I = \text{grad}\, \Phi^I$ and $\mathbb{B}^F = \text{rot}\, A^F$, where $\Phi^I = \{\varphi \in \Phi : \int_c \tau \cdot \text{grad}\, \varphi = I\}$ and $A^F = \{a \in A : \int_C n \cdot \text{rot}\, a = F\}$, the pre-images of $\mathbb{H}^I$ and $\mathbb{B}^F$.

Note these are not vector subspaces, but *affine* subspaces of $\mathbb{H}$, $\mathbb{B}$, etc., unless $I = 0$ or $F = 0$. We consistently denote by $\mathbb{H}^0$, $\mathbb{B}^0$, Φ^0, A^0 the subspaces that would be obtained in the latter case. $\mathbb{H}^I$ is *parallel*, the usual way, to $\mathbb{H}^0$, and so forth. The following lemma will be important:

Lemma 6.1. *Spaces $\mathbb{H}^0$ and $\mathbb{B}$ are* orthogonal *in* $\mathbb{L}^2(D)$, *i.e.,* $\int_D h \cdot b = 0$ *if* $h \in \mathbb{H}^0$ *and* $b \in \mathbb{B}$. *Similarly, $\mathbb{H}$ and $\mathbb{B}^0$ are orthogonal.*

Proof. Let $h \in \mathbb{H}$ and $b \in \mathbb{B}$. Then $h = \nabla\varphi$. Let φ_0 and φ_1 be the values of φ on both parts of S^h. One has $\int_D h \cdot b = \int_D b \cdot \nabla\varphi = -\int_D \varphi\ \text{div}\, b + \int_S \varphi\ n \cdot b = \int_{S^h} \varphi\ n \cdot b$ after (4), and this is equal to $(\varphi_1 - \varphi_0) \int_{S^h} n \cdot b$, that is, to the product $(\int_c \tau \cdot h)(\int_C n \cdot b)$. Now if $h \in \mathbb{H}^0$, or $b \in \mathbb{B}^0$, one of the factors vanishes. ◊

Remark 6.2. There is more, actually: With the simple topology we have here, both pairs are ortho-*complements* in $\mathbb{L}^2(D)$, which amounts to saying that any square-integrable field u can be written as $u = h + b$, with $h \in \mathbb{H}^0$ and $b \in \mathbb{B}$, or with $h \in \mathbb{H}$ and $b \in \mathbb{B}^0$, i.e., as the sum of a curl-free field and a solenoidal field. These are *Helmholtz decompositions.* We

won't need a thorough treatment of them, but the paradigm is important, and will recur. ◊

The present state of affairs is summarized by Fig. 6.2, in which one may recognize a part of the front of Maxwell's building of Fig. 5.1. Note how all "vertical" relations have been taken care of, in advance, by the very choice of functional spaces. Only the "horizontal" condition (5), which expresses the constitutive laws of materials inside D, remains to be dealt with.

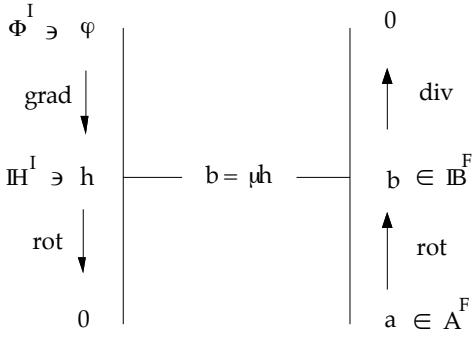

FIGURE 6.2. Structure of the magnetostatics problem. (This is a "Tonti diagram" [To]. Similar graphic conventions have been independently proposed by many researchers, Roth in particular [Rt]. See [Bw] for some history.)

6.1.2 Variational characterization of the solution

The following result will make the horizontal connection.

Proposition 6.2. *The problem which consists in finding* $h \in \mathbb{H}^I$ *and* $b \in \mathbb{B}^F$ *such that*

$$\int_D \mu^{-1} |b - \mu h|^2 \le \int_D \mu^{-1} |b' - \mu h'|^2 \quad \forall\, h' \in \mathbb{H}^I, \ \forall\, b' \in \mathbb{B}^F, \tag{9}$$

has a unique solution, which is the solution of (1–7) *when the latter exists.*

Proof. The proof of Lemma 6.1 shows that $\int_D h' \cdot b' = I\ F$. Therefore,

$$\int_D \mu^{-1} |b' - \mu h'|^2 = \int_D \mu^{-1} |b'|^2 + \int_D \mu |h'|^2 - 2\ I\ F \tag{10}$$

for all pairs $\{h', b'\} \in \mathbb{H}^I \times \mathbb{B}^F$. This means that problem (9) splits in two *independent* minimization problems:

$$\textit{find } h \in \mathbb{H}^I \textit{ such that } \int_D \mu |h|^2 \textit{ is minimum} \tag{11}$$

and

(12) *find* $b \in \mathbb{B}^F$ *such that* $\int_D \mu^{-1} |b|^2$ *is minimum.*

Both problems have a unique solution by the Hilbertian projection theorem (because $\mathbb{H}^I$ and $\mathbb{B}^F$ are closed convex sets). The minima are necessarily of the form $S I^2$ and $R F^2$, where R and S are positive constants. Then (10) shows that

$$\int_D \mu^{-1} |b - \mu h|^2 = R F^2 + S I^2 - 2 I F \geq 0$$

whatever F and I. If (1–7) has a solution for a nontrivial pair $\{I, F\}$, the left-hand side vanishes, which implies $RS = 1$ (look at the discriminant), $I = RF$, and $b = \mu h$. We call R the *reluctance* of D under the prevailing boundary conditions. ◊

We note that, for a given nonzero F, there is always a value of I such that the left-hand side of (9) vanishes, namely $I = RF$, so this proves the existence in (1–7) for the right value of I/F. However, the point of Prop. 6.2 is not to prove again the existence of a solution to the magnetostatics problem, but to introduce a new variational characterization of it. The quantity at the right-hand side of (9) is an "error in constitutive law" as regards the pair $\{h', b'\}$. Thus, compliance with such a law amounts to looking for a couple of fields that minimize the discrepancy, among those that satisfy all other required conditions. This old and esthetically attractive idea, which generalizes to *monotone* nonlinear constitutive laws, thanks to the theory of convex functions in duality [Fe, Ro], seems to date back to Moreau [Mo, Ny], and has been increasingly popular ever since (and rediscovered), in the "computational magnetics" community [R§] and others [OR, LL]. It works for *time-dependent* problems just as well [B2, A&].

There are several equivalent ways to formulate problems (11) and (12). One consists of writing the associated Euler equations, or weak formulations:

(13) *find* $h \in \mathbb{H}^I$ *such that* $\int_D \mu\ h \cdot h' = 0 \quad \forall\ h' \in \mathbb{H}^0$,

(14) *find* $b \in \mathbb{B}^F$ *such that* $\int_D \mu^{-1} b \cdot b' = 0 \quad \forall\ b' \in \mathbb{B}^0$.

Another consists of using *potentials*, thanks to (8):

(15) *find* $\varphi \in \Phi^I$ *minimizing* $\int_D \mu\ |\text{grad}\ \varphi|^2$,

(16) *find* $a \in A^F$ *minimizing* $\int_D \mu^{-1} |\text{rot}\ a|^2$.

Now, of course, neither φ nor a need be unique. Equivalent weak formulations are

(17) *find* $\varphi \in \Phi^{I}$ *such that* $\int_D \mu \, \mathrm{grad}\, \varphi \cdot \mathrm{grad}\, \varphi' = 0 \quad \forall \varphi' \in \Phi^{0}$,

(18) *find* $a \in A^{F}$ *such that* $\int_D \mu^{-1} \, \mathrm{rot}\, a \cdot \mathrm{rot}\, a' = 0 \quad \forall a' \in A^{0}$.

Dualizing the constraints (6) and (7), as in Exer. 2.9, is also an option, which leads to

(11') *find* $h \in \mathbb{H}$ *such that* $\int_D \mu \, |h|^2 - 2\,F\,\mathcal{J}(h)$ *is minimum,*

(12') *find* $b \in \mathbb{B}$ *such that* $\int_D \mu^{-1} \, |b|^2 - 2\,I\,\mathcal{F}(b)$ *is minimum,*

with again associated Euler equations and equivalent formulations with potentials $\varphi \in \Phi$ and $a \in A$, similar to (15)–(18).

6.1.3 Complementarity, hypercircle

At this stage, we have recovered the variational formulation in φ, Eq. (15), and derived the other one, on the "curl side", in a strictly symmetrical way. This is an encouragement to proceed in a similarly parallel fashion at the discrete level.

So let Φ_m be the subspace of mesh-wise affine functions in Φ (recall they are constant over both parts of S^h). Likewise, let's have Φ^{I}_m and Φ^{0}_m as Galerkin subspaces for Φ^{I} and Φ^{0} (with, again, the now-standard caveat about variational crimes and polyhedral domains). As in Chapter 3, we replace Problem (15) by the approximation

(19) *find* $\varphi_m \in \Phi^{I}_m$ *minimizing* $\int_D \mu \, |\mathrm{grad}\, \varphi|^2$,

which is equivalent to

(20) *find* $\varphi_m \in \Phi^{I}_m$ *such that* $\int_D \mu \, \mathrm{grad}\, \varphi_m \cdot \mathrm{grad}\, \varphi' = 0 \quad \forall \varphi' \in \Phi^{0}$.

There is a tiny difference in the present treatment, however: Observe that the solution is not unique! An additive constant has yet to be chosen, which can be achieved by, for instance, imposing $\boldsymbol{\varphi}_n = 0$ for those nodes n that lie in S^h_0, and this is most often done, without even thinking about it. So did we in Chapter 3. But this time, I *do* want to call attention on this "gauge-fixing" procedure, trivial as it is in this case.

Since the minimization in (19) is performed on a smaller space than in (17), the minimum achieved is an upper estimate of the true one: $I^2/\underline{R}_m$

instead of I^2/R, with $I^2/\underline{R}_m \geq I^2/R$, hence $\underline{R}_m \leq R$. Solving (19) or (20) thus yields a *lower bound* for the reluctance.

Now, it would be nice to have an *upper* bound as well! If we could perform the same kind of Galerkin approximation on the "vector potential" version of the problem, (16) or (18), we would indeed have one: For if A^F_m is some finite dimensional subspace of A^F, solving either the quadratic optimization problem,

$$(21) \qquad find\ a_m \in A^F_m\ minimizing \int_D \mu^{-1} |\operatorname{rot} a|^2,$$

in terms of still to be defined degrees of freedom, or the associated linear system,

$$(22) \qquad find\ a_m \in A^F_m\ such\ that \int_D \mu^{-1} \operatorname{rot} a_m \cdot \operatorname{rot} a' = 0 \quad \forall\ a' \in A^0_m,$$

will yield an upper bound $\overline{R}_m F^2$ to RF^2. Hence the bilateral estimate

$$(23) \qquad \underline{R}_m \leq R \leq \overline{R}_m,$$

obviously a very desirable outcome. This is *complementarity*, as usually referred to in the literature [Fr, HP, PF].

There is more to it. Suppose one has solved both problems (19) and (21), and let us set

$$E(b_m, h_m) = \int_D \mu^{-1} |b_m - \mu\, h_m|^2 \equiv \int_D \mu^{-1} |\operatorname{rot} a_m - \mu \operatorname{grad} \varphi_m|^2.$$

Be well aware that I and F are unrelated, a priori (we'll return to this later), so even for the exact solutions h and b of (11) and (12), the error in constitutive law $E(b, h)$ does not vanish. Thus $E(b_m, h_m)$, obtained by minimizing on finite dimensional subspaces, will be even larger. Now,

Proposition 6.3. *One has*

$$\begin{aligned} E(b_m, h_m) &= \int_D \mu^{-1} |b_m - b + b - \mu\, h + \mu(h - h_m)|^2 \\ &= \int_D \mu^{-1} |b_m - b|^2 + \int_D \mu^{-1} |b - \mu\, h|^2 + \int_D \mu\, |h - h_m|^2, \end{aligned} \qquad (24)$$

Proof. Develop the first line and observe that all rectangle terms vanish, because of a priori orthogonality relations which Fig. 6.3 should help visualize. Indeed, $b_m - b$ and $h_m - h$ belong to $\operatorname{rot} A^0 \equiv \mathbb{B}^0$ and $\operatorname{grad} \Phi^0 \equiv \mathbb{H}^0$, which are orthogonal by Lemma 6.1. This disposes of the term $\int_D \mu^{-1} (b_m - b) \cdot (\mu\, (h - h_m))$. As for $\int_D \mu^{-1} (b - \mu\, h) \cdot (\mu\, (h - h_m)$, this is equal to $\int_D (b - \mu\, h) \cdot \operatorname{grad} \psi$ for some $\psi \in \Phi^0$, which vanishes because both b and μh are solenoidal. Same kind of argument for the third term $\int_D (b_m - b) \cdot (\mu^{-1} b - h)$, because $\operatorname{rot} h = 0$ and $\operatorname{rot}(\mu^{-1} b) = 0$. ◊

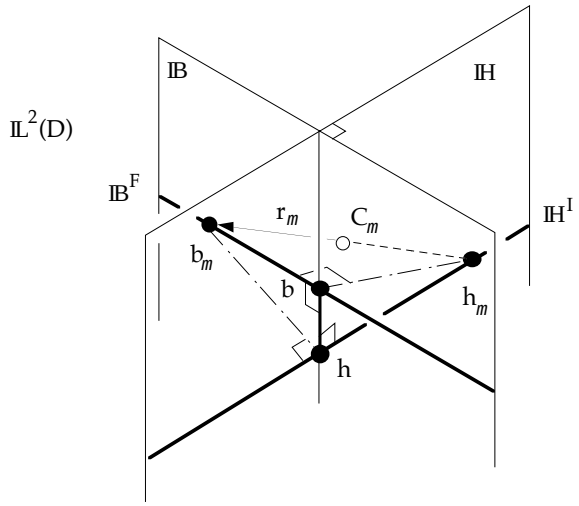

FIGURE 6.3. The geometry of complementarity. All right angles in sight, marked by carets, do correspond to orthogonality properties, in the sense of the scalar product of $\mathbb{L}^2(D)$, which result from Lemma 6.1 and from variational characterizations. (All $\mathbb{B}^F$s [resp. all $\mathbb{H}^I$s] are orthogonal to $\mathbb{H}$ [resp. to $\mathbb{B}$].) Note how h, h_m, b, b_m, all stand at the same distance r_m from $C_m = (h_m + b_m)/2$, on a common "hypercircle", and how the equality (24) can be read off the picture. For readability, this is drawn as if one had $\mu = 1$, but all geometric relations stay valid if all symbols h and $\mathbb{H}$ [resp. b and $\mathbb{B}$] are replaced by $\mu^{1/2} h$ and $\mu^{1/2} \mathbb{H}$ [resp. by $\mu^{-1/2} b$ and $\mu^{-1/2} \mathbb{B}$].

Since $E(b_m, h_m) = \int_D \mu^{-1} |b_m - \mu h_m|^2 \equiv \sum_{T \in \mathcal{T}} \int_T \mu^{-1} |b_m - \mu h_m|^2$ is a readily computable quantity, (24) stops the gap we had to deplore in Chapter 4: *At last, we have a posteriori bounds* on the approximation errors[4] for both h_m and b_m, which appear in first and third position at the right-hand side of (24). All it requires is to solve for *both* potentials φ and a, by some Galerkin method. Of course, the smaller the middle term $E(b, h)$, the sharper the bounds, so I and F should not be taken at random. For efficiency, one may set I, get φ_m, evaluate the flux F by the methods of Chapter 4 (cf. Subsection 4.1.3, especially Fig. 4.7), and finally, compute a_m for *this* value of the flux.

Exercise 6.1. Show that this procedure is actually optimal, giving the sharpest bound for a given I.

[4]Global bounds, not local: It is not necessarily true that $E_T(b_m, h_m)$, that is, $\int_T \mu^{-1} |b_m - \mu h_m|^2$, is an upper bound for $\int_T \mu^{-1} |b - b_m|^2$ and $\int_T \mu |h - h_m|^2$. Still, it's obviously a good idea to look for tetrahedra T with relatively high E_T, and to refine the mesh at such locations. Cf. Appendix C.

Remark 6.3. As Fig. 6.3 suggests, the radius r_m of the hypercircle is given by $[E(b_m, h_m)]^{1/2}/2$. This information allows one to get bilateral bounds on other quantities than the reluctance. Suppose some quantity of interest is a linear continuous functional of (say) h, L(h). There is a Riesz vector h^L for this functional (cf. A.4.3), such that $L(h) = \int_D \mu\, h^L \cdot h$. What is output is $L(h_m)$. But one has $|L(h) - L(h_m)| = |\int_D \mu\, h^L \cdot (h - h_m)| \le \|h^L\|_\mu \|h - h_m\|_\mu \le r_m \|h^L\|_\mu$, hence the bounds. There is a way to express the value of the potential at a point x as such a functional [Gr]. Hence the possibility of *pointwise* bilateral estimates for the magnetic potentials. This was known long ago (see bibliographical comments at the end), but seems rarely applied nowadays, and some revival of the subject would perhaps lead to interesting applications. ◊

6.1.4 Constrained linear systems

With such incentives, it becomes almost mandatory to implement the vector potential method. All it takes is some Galerkin space A^F_m, and since the unknown a is *vector*-valued, whereas φ was *scalar*-valued, let's pretend we don't know about edge elements and try this: Assign a *vector-valued* DoF $\underline{\mathbf{a}}_n$ to each node, and look for the vector field a as a linear combination

$$a = \sum_{n \in \mathcal{N}} \underline{\mathbf{a}}_n w_n.$$

(We shall have to refer to the space spanned by such fields later, so let us name it $\mathbb{P}^1_m$, on the model of the P^1 of Chapter 3, the "blackboard" style reminding us that each DoF is a vector.) Now (21) is a quadratic optimization problem in terms of the Cartesian components of the vector DoFs. The difficulty is, these degrees of freedom are not *independent*, because a must belong to A^F_m. As such, it should first satisfy $n \cdot \mathrm{rot}\, a = 0$ on S^b, that is, on each face f of the mesh that belongs to S^b. Assume again flat faces, for simplicity, and let n_f be the normal to f. Remembering that $\mathcal{N}(f)$ denotes the subset of nodes that belong to f, we have, on face f,

$$n \cdot \mathrm{rot}\, a = \sum_{v \in \mathcal{N}(f)} n_f \cdot \mathrm{rot}(\underline{\mathbf{a}}_v\, w_v) = \sum_{v \in \mathcal{N}(f)} n_f \cdot (\nabla w_v \times \underline{\mathbf{a}}_v)$$
$$\equiv \sum_{v \in \mathcal{N}(f)} (n_f \times \nabla w_v) \cdot \underline{\mathbf{a}}_v\,,$$

since $n \times \nabla w_v$ vanishes for all other nodes v (Fig. 6.4), hence the linear constraints to be verified by the DoFs:

$$\sum_{v \in \mathcal{N}(f)} (n_f \times \nabla w_v) \cdot \underline{\mathbf{a}}_v = 0$$

for each face f in S^b. The condition on the flux, $\int_C n \cdot \mathrm{rot}\, a = F$, will also yield such a constraint. Taken all together, these constraints can be expressed as $\mathbf{L}\,\mathbf{a} = F\,\mathbf{k}$, where $\mathbf{L}$ is some rectangular matrix and $\mathbf{k}$ a fixed vector. (We shall be more explicit later about $\mathbf{L}$ and $\mathbf{k}$. Just note that entries of $\mathbf{L}$ are not especially simple, not integers at any rate, and frame-dependent.)

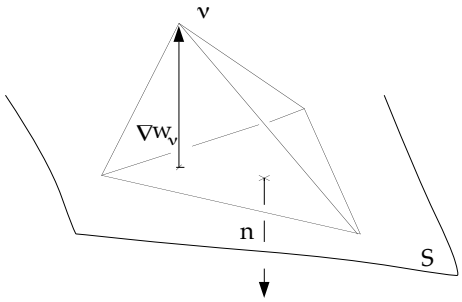

FIGURE 6.4. All surface fields $n \times \nabla w_\nu$ vanish, except when node ν belongs to the boundary.

To sum up: The quadratic optimization problem (21) is more complex than it would appear. Sure, the quantity to be minimized is a quadratic form in terms of the vector $\mathbf{a}$ of DoFs (beware, this is a vector of dimension 3N, if there are N nodes):

$$\int_D \mu^{-1} \,|\, \mathrm{rot}\, a \,|^2 = (\mathbf{M}\,\mathbf{a}, \mathbf{a}),$$

if we denote by $\mathbf{M}$ the associated symmetric matrix. But $(\mathbf{M}\,\mathbf{a}, \mathbf{a})$ should be minimized *under the constraint* $\mathbf{L}\,\mathbf{a} = F\,\mathbf{k}$, so the components of $\mathbf{a}$ are not *independent* unknowns.

Problems of this kind, that we may dub *constrained linear systems*, happen all the time in numerical modelling, and there are essentially two methods to deal with them. Both succeed in removing the constraints, but one does so by increasing the number of unknowns, the other one by decreasing it.

The first method[5] consists in introducing Lagrange multipliers: minimize the Lagrangian $(\mathbf{M}\,\mathbf{a}, \mathbf{a}) + 2(\boldsymbol{\lambda}, \mathbf{L}\,\mathbf{a})$ with respect to $\mathbf{a}$, without constraints, and adjust the vector of multipliers $\boldsymbol{\lambda}$ in order to enforce $\mathbf{L}\,\mathbf{a} = F\,\mathbf{k}$. This amounts to solving the following augmented linear system, in block form:

[5]Often referred to as the "dualization of constraints", a systematic application of the trick we encountered earlier in Exer. 2.9.

$$\begin{vmatrix} \mathbf{M} & \mathbf{L}^t \\ \mathbf{L} & 0 \end{vmatrix} \begin{vmatrix} \mathbf{a} \\ \boldsymbol{\lambda} \end{vmatrix} = \mathrm{F} \begin{vmatrix} 0 \\ \mathbf{k} \end{vmatrix}. \tag{25}$$

This is what is called, according to a rather dubious but already entrenched terminology, a *mixed system*. It's a standard (unconstrained) symmetric linear system, but deprived of properties such as positive definiteness, so solving (25) is a challenge for which classical matrix analysis did not prepare us. See Appendix B for a few directions.

Exercise 6.2. What is the physical interpretation of the components of $\boldsymbol{\lambda}$?

The second method consists in expressing all unknowns in terms of a well-chosen set of independent variables. These may or may not coincide with a subset of the original unknowns. Most often they do, and picking the independent ones is so easy and so natural that one is not even aware of doing it. This is the case with Problem (19) or (20) above. Set in terms of $\boldsymbol{\varphi}$, (19) is actually a constrained linear system, the constraints on $\boldsymbol{\varphi}$ being as follows: (1) all $\boldsymbol{\varphi}_n$ for n in S^h_0 equal to some constant, (2) all those for n in S^h_1 equal to some other constant, and (3) the difference between these constants being equal to I. This can be compactly written as $\mathbf{L}\boldsymbol{\varphi} = \mathrm{I}\,\mathbf{k}$, just as before (with, of course, a different $\mathbf{L}$ and a different $\mathbf{k}$), and one could imagine using Lagrange multipliers. But it's much easier to set $\boldsymbol{\varphi}_n = 0$ for all n in S^h_0 (one will recognize the previous "gauge fixing" in action there), $\boldsymbol{\varphi}_n = \mathrm{I}$ for all n in S^h_1, and to solve with respect to other, obviously independent, nodal DoFs. So this is an example of a constrained linear system for which the sifting of dependent variables is straightforward.

Unfortunately, such is not the case with (21) or (22). The only recourse is to extract from $\mathbf{L}$ a submatrix of maximum rank (there do exist algorithms for this purpose [AE]), and thus to select independent variables to solve for. But this is a costly process. So the vector potential approach to magnetostatics looks unappealing, a priori.

6.2 SOLVING THE MAGNETOSTATICS PROBLEM

Should we then renounce the benefits of complementarity? No, thanks to edge elements.

6.2.1 Embedding the problem in Maxwell–Whitney's house

In fact, after Chapter 5, it's hard *not* to think of edge elements in the present context. We know, by Fig. 6.2, how the present problem fits within Maxwell's "continuous" building, so all we have to do is *embed* it in the relevant part of the Maxwell–Whitney "discrete" building. To make this formal, let us introduce a few definitions: Just as Φ^I_m above is the intersection $W^0_m \cap \Phi^I$, let us set $\mathbb{H}^I_m = W^1_m \cap \mathbb{H}^I$, as well as $\mathbb{B}^F_m = W^2_m \cap \mathbb{B}^F$ and—now committing ourselves to a definite approximation space— $A^F_m = W^1_m \cap A^F$. This is a sensible move, since elements of $\mathbb{H}^I_m$ and $\mathbb{B}^F_m$ have the kind of continuity required from h and b respectively, and the representations by potentials work nicely: indeed, grad $\Phi^I_m = \mathbb{H}^I_m$ and rot $A^F_m = \mathbb{B}^F_m$.

Any pair {h, b} taken in $\mathbb{H}^I_m \times \mathbb{B}^F_m$ will thus satisfy all equations (1–7) except $b = \mu h$, the constitutive law. The latter cannot hold, since W^1_m and W^2_m are different spaces (and by the no-free-lunch principle we had to apply once already: *all* equations cannot *exactly* be satisfied when we discretize). Hence the question mark in the center of Fig. 6.5.

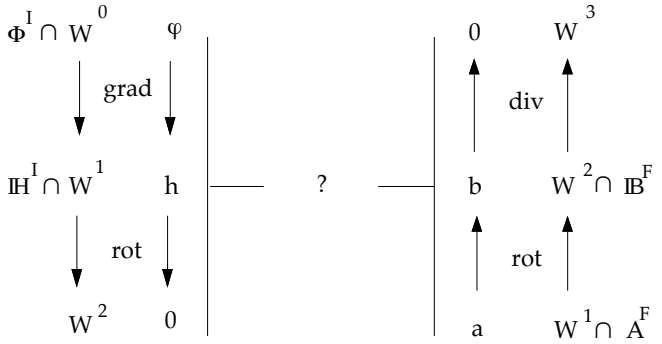

FIGURE 6.5. Two copies of the top sequence of (5.13), put vertically, one downwards, one upwards, and appropriately clipped, form a framework in which Fig. 6.2 can be embedded, except for the horizontal relation, which must be relaxed.

So we settle for the next best thing, which is to minimize the error in constitutive law: *find* $h_m \in \mathbb{H}^I_m$ *and* $b_m \in \mathbb{B}^F_m$ *such that*

$$\int_D \mu^{-1} |b_m - \mu h_m|^2 \le \int_D \mu^{-1} |b' - \mu h'|^2 \quad \forall h' \in \mathbb{H}^I_m, \ \forall b' \in \mathbb{B}^F_m,$$

and for exactly the same reasons as in Prop. 6.2, this splits into a pair of independent problems:

(26) *find* $h_m \in \mathbb{H}^I_m$ *minimizing* $\int_D \mu\, |h|^2$,

(27) *find* $b_m \in \mathbb{B}^F_m$ *minimizing* $\int_D \mu^{-1}\, |b|^2$.

To investigate the algebraic nature of these problems, let us express them in terms of degrees of freedom. (Recall the generic notation $\mathcal{E}(\ldots)$ or $\mathcal{F}(\ldots)$ for the sets of edges or faces that belong to some region of space or to some geometric element (surface, line . . .) whose name stands inside the parentheses.) We assume the link c and the cut C of Fig. 6.1 are unions of edges and faces of the mesh. By analogy with the incidence numbers $\mathbf{R}_{f\,e}$, let us have $\mathbf{R}_{c\,e} = \pm 1$ if edge e belongs to c, the sign being plus if their orientations match, and $\mathbf{R}_{c\,e} = 0$ otherwise. Similarly, let $\mathbf{D}_{C\,f} = \pm 1$ if face f belongs to C, with the same sign convention, and 0 otherwise. We may now define

$$\mathbf{H}^I = \{\mathbf{h} \in \mathbf{W}^1 :\ \mathbf{h}_e = 0\ \ \forall\, e \in \mathcal{E}(S^h),\ \ \textstyle\sum_{e \in \mathcal{E}(c)} \mathbf{R}_{c\,e}\, \mathbf{h}_e = I\},$$

$$\mathbf{B}^F = \{\mathbf{b} \in \mathbf{W}^2 :\ \mathbf{b}_f = 0\ \ \forall\, f \in \mathcal{F}(S^b),\ \ \textstyle\sum_{f \in \mathcal{F}(C)} \mathbf{D}_{C\,f}\, \mathbf{b}_f = F\},$$

and using the mass matrices of Chapter 5, problems (26) and (27) are equivalent to

(28) *find* $\mathbf{h} \in \mathbf{H}^I$ *such that* $(\mathbf{M}_1(\mu)\, \mathbf{h}, \mathbf{h})$ *is minimum,*

(29) *find* $\mathbf{b} \in \mathbf{B}^F$ *such that* $(\mathbf{M}_2(\mu^{-1})\, \mathbf{b}, \mathbf{b})$ *is minimum,*

two "constrained linear systems", according to the foregoing terminology. Solving both will give the bilateral estimate (23) of the reluctance.

As constrained linear systems, problems (28) and (29) can be attacked by both general strategies: (1) introduce Lagrange multipliers, hence the so-called "mixed" formulations (and though not very popular, some of them have been tried; see, e.g., [PT]), or (2) select independent variables. For this second strategy, there are again two variants. Independent variables can just be picked among the original ones, and this is what spanning tree extraction techniques permit (cf. Fig. 6.6), hence numerical methods in terms of h and b directly. Both have been considered [Ke]. (The one in b seems less robust [Ke], and it would be worthwhile to understand why.) The second variant corresponds to the introduction of potentials: node or edge variables that help represent the above h and b, while automatically taking constraints into account.

Thus treated, (26) and (27) become

(30) *find* $\varphi_m \in \Phi^I_m$ *such that* $\int_D \mu\, |\mathrm{grad}\, \varphi|^2$ *is minimum,*

(31) *find* $a_m \in A^F_m$ *such that* $\int_D \mu^{-1} |\,\mathrm{rot}\, a\,|^2$ *is minimum,*

and in terms of degrees of freedom,

(32) *find* $\boldsymbol{\varphi} \in \boldsymbol{\Phi}^I$ *such that* $(\mathbf{M}_1(\mu)\, \mathbf{G}\boldsymbol{\varphi}, \mathbf{G}\boldsymbol{\varphi})$ *is minimum,*

(33) *find* $\mathbf{a} \in \mathbf{A}^F$ *such that* $(\mathbf{M}_2(\mu^{-1})\, \mathbf{R}\mathbf{a}, \mathbf{R}\mathbf{a})$ *is minimum,*

where $\boldsymbol{\Phi}^I = \{\boldsymbol{\varphi} \in \mathbf{W}^0 : \mathbf{L}\boldsymbol{\varphi} = I\,\mathbf{k}\}$ has already been described, for system (32) is nothing else than the scalar potential method of Chapter 3. The novelty is (33), which realizes (at last!) the discretization "on the curl side" of Eqs. (2.20) to (2.26).

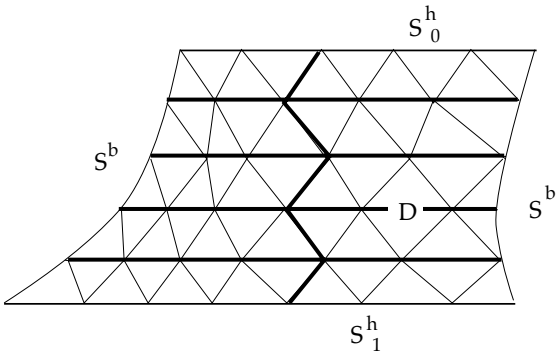

FIGURE 6.6. Tree of edges for the model problem in dimension 2. (This is actually a "belted tree mod S^h" in the language of Section 5.3.) Note how all edge circulations of h are determined by those of the tree edges (in thick lines), thanks to $\mathrm{rot}\, h = 0$ (cf. Fig. 5.5) and $n \times h = 0$ on S^h.

So let us look at $\mathbf{A}^F$, or equivalently, at the associated space of fields, A^F_m. Elements of the latter are subject to the conditions $n \cdot \mathrm{rot}\, a = 0$ over each face f in S^b and $\int_C n \cdot \mathrm{rot}\, a = F$. Since $\mathrm{rot}\, a$ is mesh-wise constant, $n \cdot \mathrm{rot}\, a = 0$ over f results in one relation between the $\mathbf{a}_e$s, namely $\sum_{e \in \mathcal{E}} \mathbf{R}_{f\,e}\, \mathbf{a}_e = 0$, which involves only the DoFs of the three edges that bound f (the trick of Fig. 5.5, again). The condition on the flux through C results in a similar relation: $\sum_{e \in \mathcal{E}(\partial C)} \mathbf{R}_{\partial C\, e}\, \mathbf{a}_e = F$, where $\mathbf{R}_{\partial C\, e} = \pm 1$, depending on the orientation of edge e relative to ∂C. Taken all together, the constraints can thus be expressed as $\mathbf{L}\,\mathbf{a} = F\,\mathbf{k}$, just as in the case of nodal vectorial elements, but $\mathbf{L}$ is now much simpler, with entries ± 1 or 0 that are obtained by simply looking at how edges are oriented. This is a considerable improvement.

Still, these constraints are in the way, and whether we can get rid of them simply is the litmus test that will, if passed, establish the superiority of edge elements in the vector potential approach.

6.2.2 Dealing with the constraints

Indeed, the constraints can be removed by the following method. First construct a special DoF vector $\mathbf{a}^F$, such that the associated field $a^F = \sum_{e \in \mathcal{E}} \mathbf{a}^F{}_e w_e$ belong to A^F. This will be done in the next paragraph. Then, instead of minimizing over all $A^F{}_m$, we shall do it over fields of the form $a^F + \sum \mathbf{a}_e w_e$, where the index e spans $\mathcal{E} - \mathcal{E}(S^b)$, i.e., without any restriction on the $\mathbf{a}_e$s, but excluding edges of S^b. Edge DoFs in this summation are now *independent*. The final version of the problem will thus be: *find* $\mathbf{a} \in \tilde{\mathbf{A}}^F$ *such that* $(\mathbf{M}_2(\mu^{-1})\ \mathbf{Ra},\ \mathbf{Ra})$ *be minimum,* where $\tilde{\mathbf{A}}^F$ is the subset $\{\mathbf{a} \in \mathbf{W}^1 :\ \mathbf{a}_e = \mathbf{a}^F{}_e\ \forall\ e \in \mathcal{E}(S^b)\}$, which amounts to solving a linear system with respect to the DoFs of the "inner edges" (those not in S^b).

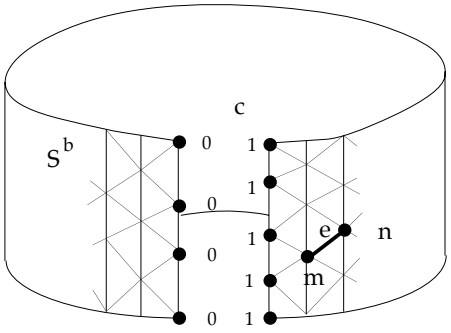

FIGURE 6.7. One step in the construction of $\mathbf{a}^F$: assigning scalar values to nodes on the boundary S^b, after having doubled the nodes on the "cut" c.

The construction of $\mathbf{a}^F$ proceeds as follows (Fig. 6.7). Consider the mesh of surface S^b, as induced by *m*. Make a (one-dimensional) "cut" c by following a path of edges from top to bottom. Double the nodes along c. Assign scalar values $\mathbf{v}_n$ to nodes, arbitrary values, except for the pairs of nodes along c, that should receive zeroes and ones, on the pattern suggested by Fig. 6.7. Then, assign to all edges $e = \{m, n\}$ the value $\mathbf{a}^F{}_e = (\mathbf{v}_n - \mathbf{v}_m)F$ if $e \in \mathcal{E}(S^b)$, $\mathbf{a}^F{}_e = 0$ otherwise. The recipe works because, whatever $a = \sum\{e \in \mathcal{E} :\ \mathbf{a}_e w_e\}$ in $A^F{}_m$, there is a modified field $\tilde{a} = \sum_{e \in \mathcal{E}} \tilde{\mathbf{a}}_e w_e$, where $\tilde{\mathbf{a}}_e = \mathbf{a}^F{}_e$ if $e \notin \mathcal{E}(S^b)$ and $\tilde{\mathbf{a}}_e = \mathbf{a}_e$ otherwise (hence $\tilde{\mathbf{a}} \in \tilde{\mathbf{A}}$), *that has the same curl* as a (this is the point of the above construction). Thus, one minimizes in (31) over a space $\tilde{A}^F{}_m$ strictly smaller than $A^F{}_m$, but with $\mathrm{rot}\, A^F{}_m = \mathrm{rot}\, \tilde{A}^F{}_m$ $(\equiv \mathbb{B}^F{}_m)$, so the same b is reached.

Remark 6.4. As the kernel $\ker(\mathbf{R};\ \tilde{\mathbf{A}}) = \{\mathbf{a} \in \tilde{\mathbf{A}} :\ \mathbf{Ra} = 0\}$ does not reduce to 0, this final version of the vector potential approach does not give a unique

a, although a unique b is obtained. The associated linear system is therefore singular. We shall return to this apparent difficulty. ◊

6.2.3 "*m*-weak" properties

We should now proceed as in Section 4.1, and answer questions about the quality of the approximation provided by a_m: We are satisfied that $b_m = \text{rot}\, a_m$ is solenoidal and that $n \cdot b_m = 0$ on the S^b boundary, but what is left of the "weak irrotationality" of $h_m = \mu^{-1} b_m$? And so forth.

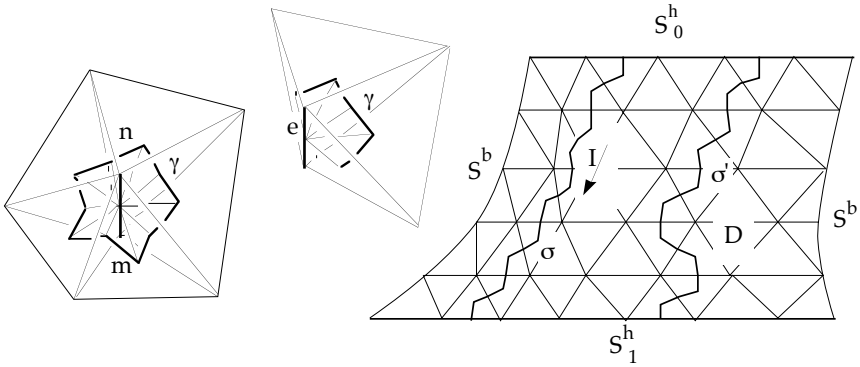

FIGURE 6.8. "*m*-weak" properties of the vector potential solution. Left: The circulation of $h_m = \mu^{-1}\,\text{rot}\, a_m$ is zero along the circuit γ that joins barycenters around any inner edge $e = \{m, n\}$. Middle: If e belongs to S^h, the circulation is null along the open path γ. Right: The "variationally correct" mmf is obtained by taking the circulation of the computed h_m along the "*m**-line" σ joining S^h_0 and S^h_1, or along any homologous *m**-line σ'.

It would be tedious to go through all this again, however, and there is more fun in *guessing* the results, thanks to the analogies that Tonti's diagrams so strongly suggest. So we can expect with confidence the following statements to be true:

- For any DoF vector $\mathbf{a}$, the term $(\mathbf{R}^t\mathbf{M}_2(\mu^{-1})\,\mathbf{R}\mathbf{a})_e \equiv \int_D h \cdot \text{rot}\, w_e$, where $h = \mu^{-1}\,\text{rot}(\sum_{e \in \mathcal{E}} \mathbf{a}_e w_e)$, is the circulation of h along the smallest closed *m**-line (closed mod S, in the case of surface edges) that surrounds edge e (cf. Fig. 6.8).

- The circulation of the computed field, h_m, vanishes along all *m**-lines which bound modulo S^h (cf. Fig. 4.6, right).

- The circulation of h_m is equal to I along all *m**-paths similar to σ (or its homologue σ') on Fig. 6.8.

Exercise 6.3. Prove all this.

There is more to say about complementarity. In particular, there is an obvious problem of duplication of efforts: Computations of φ and a are independent, though their results are closely related. No use is made of the knowledge of φ when solving for a, which seems like a waste, since as one rightly suspects, and as the following discussion will make clear, solving for a is much more expensive than solving for φ. There is a way to save on this effort, which is explained in detail in Appendix C. We now address the more urgent question of whether edge elements are really mandatory in the vector potential approach.

6.3 WHY NOT STANDARD ELEMENTS ?

As we saw, edge elements are able to solve a problem that was quite difficult with nodal vectorial elements, namely, to obtain a vector potential formulation in terms of explicit *independent* degrees of freedom. This is a good point, but not the whole issue, for difficult does not mean impossible, and if bilateral estimates, or any other consequence of the hypercircle trick, are the objective, one must concede that it *can* be achieved with standard nodal elements, scalar-valued for φ, vector-valued for a. All that is required is approximation "from inside" (within the functional space), Galerkin style. It's thus a gain in simplicity or in accuracy, or both, that we may expect of edge elements.

To make a fair comparison, let us suppose that, after proper selection of independent variables, the vector potential approach with nodal elements consists in looking for a in some subspace of $\mathbb{P}^1{}_m$, that we shall denote $\tilde{A}^F{}_m(\mathbb{P}^1)$. Let us similarly rename $\tilde{A}^F{}_m(W^1)$ the above $\tilde{A}^F{}_m$, to stress its relationship with edge elements. In both methods, the quantity $\int_D \mu^{-1} |\operatorname{rot} a|^2$ is minimized, but on different subspaces of $\mathbb{L}^2{}_{\text{rot}}(D)$, which results in linear systems of the same form $\mathbf{Ma} = \mathbf{b}$, but with different $\mathbf{M}$ and $\mathbf{b}$, and a different interpretation for the components of $\mathbf{a}$. Let us call $\mathbf{M}_P$ and $\mathbf{M}_W$, respectively, the matrix $\mathbf{M}$ in the case of the $\mathbb{P}^1$ and the W^1 approximation. Both are symmetric and (a priori) nonnegative definite. We shall find the nodal vectorial approach inferior on several counts. But first . . .

6.3.1 An apparent advantage: $\mathbf{M}_P$ is regular

Indeed, let $a \in \tilde{A}^F{}_m(\mathbb{P}^1)$ be such that $\operatorname{rot} a = 0$, which is equivalent to $\mathbf{Ma} = 0$. Then $a = \operatorname{grad} \psi$. Since a is piecewise linear with respect to the

mesh m a*nd* continuous (in all its three scalar components), φ is piecewise quadratic *and* differentiable, two hardly compatible conditions. The space P^2 of piecewise quadratic functions on m is generated by the products $w_n w_m$, where n and m span the nodal set $\mathcal{N}$. Therefore, grad $\psi = \sum_{m,n \in \mathcal{N}} \alpha_{mn} \text{grad}(w_m w_n)$, and since the products $w_n w_m$ are not differentiable, the normal component of this field has a nonzero jump across all faces. (This jump is affine with respect to coordinates over a face.) Demanding that all these jumps be 0 is a condition that considerably constrains the α's (in practice, only globally quadratic ψ, as opposed to mesh-wise quadratic, will comply). Consequently, the kernel of rot in $\tilde{A}^F_m(\mathbb{P}^1)$ will be of very low dimension, and as a rule reduced to 0, because of additional constraints imposed by the boundary conditions. So unless the mesh is very special, one may expect a regular $\mathbf{M}_P$, whereas the matrix $\mathbf{M}_W$ is singular, since W^1 contains gradients (cf. Prop. 5.4, asserting that $W^1 \supset \text{grad } W^0$).

Good news? We'll see. Let us now look at the weak points of the nodal vectorial method.

6.3.2 Accuracy is downgraded

When working with the same mesh, accuracy is downgraded with nodal elements, because $\text{rot}(\tilde{A}^F_m(\mathbb{P}^1)) \subset \text{rot}(\tilde{A}^F_m(W^1))$, with as a rule a *strict* inclusion. Minimizing over a smaller space will thus yield a less accurate upper bound in the case of nodal elements, for a given mesh m. (Let's omit the subscript m for what follows, as far as possible. Recall that N, E, F, T refer to the number of nodes, etc., in the mesh.)

The inclusion results from this:

Proposition 6.4. *For a given mesh m, any field $u \in \mathbb{P}^1$ is sum of some field in W^1 and of the gradient of some piecewise quadratic function, i.e.,*

$$\mathbb{P}^1 \subset W^1 + \text{grad } P^2.$$

Proof. Given $u \in \mathbb{P}^1$, set $\mathbf{u}_e = \int_e \tau \cdot u$, for all $e \in \mathcal{E}$, and let $v = \sum_{e \in \mathcal{E}} \mathbf{u}_e w_e$ be the field in W^1 which has these circulations as edge DoFs. Then, both u and v being linear with respect to coordinates, rot(u – v) is piecewise constant. But its fluxes through faces are 0, by construction (again, see Fig. 5.5), so it vanishes. Hence $u = v + \nabla\varphi$, where φ is such that $\nabla\varphi$ be piecewise linear, that is, $\varphi \in P^2$. ◊

As a corollary, $\text{rot } \mathbb{P}^1 \subset \text{rot } W^1$, hence the inclusion, as far as (but this is what we assumed for fairness) $\tilde{A}^F_m(\mathbb{P}^1) \subset A^F$. As a rule, this is strict inclusion, because the dimension of $\text{rot } \mathbb{P}^1$ cannot exceed that of $\mathbb{P}^1$, which

is $3N$ (three scalar DoFs per node), whereas the dimension of $\mathrm{rot}\, W^1$ is (approximately the same as) that of the quotient $W^1/\mathrm{grad}(W^0)$, which is $E - N + 1$, that is, 5 to 6 N, depending on the mesh, as we know (cf. 4.1.1).

Exercise 6.4. Check that $\mathbb{P}^1$ is *not* contained in W^1.

Exercise 6.5. Show that $W^1 \subset \mathbb{P}^1 + \mathrm{grad}\, P^2$ does *not* hold.

6.3.3 The "effective" conditioning of the final matrix is worsened

The importance of the *condition number* of a matrix, that is, the ratio of its extreme eigenvalues, is well known. This number determines to a large extent the speed of convergence of iterative methods of solution, and the numerical accuracy of direct methods.

This is true, that is, in the case of *regular* matrices. But if a symmetric nonnegative definite matrix $\mathbf{M}$ is singular, this does not preclude the use of iterative methods to solve $\mathbf{Ma} = \mathbf{f}$. All that is required is that $\mathbf{f}$ be in the range of $\mathbf{M}$, so that $(\mathbf{Ma}, \mathbf{a}) - 2(\mathbf{f}, \mathbf{a})$ have a finite lower bound. Then any "descent" method (i.e., one that tries to minimize this function by decreasing its value at each iteration) will yield a minimizing sequence $\mathbf{u}_k$ that may not converge, but *does converge modulo* $\ker(\mathbf{M})$, and this may be just enough. To be definite, suppose the matrix $\mathbf{M}$ is a principal submatrix of $\mathbf{R}^t\mathbf{M}(\mu^{-1})\mathbf{R}$, as was shown to be the case with edge elements. The quadratic form to be minimized is indeed bounded from below, and the desired convergence is that of $\mathbf{Ra}_k$, not $\mathbf{a}_k$. By working out the simple example of the iterative method $\mathbf{u}_{n+1} = \mathbf{u}_n - \rho\,(\mathbf{Ma}_n - \mathbf{f})$, which is easy in the basis of eigenvectors of $\mathbf{M}$, one will see that what counts, as far as convergence modulo $\ker(\mathbf{M})$ is concerned, is the ratio of extreme strictly positive eigenvalues. Let us call this *effective* conditioning, denoted by $\kappa(\mathbf{M})$.

We now show that $\kappa(\mathbf{M}_P) >> \kappa(\mathbf{M}_W)$, thus scoring an important point for edge elements. This will be quite technical, unfortunately.

Both matrices can be construed as approximations of the "curl–curl" operator, $\mathrm{rot}(\mu^{-1}\,\mathrm{rot}\,)$, or rather, of the associated boundary-value problem. Their higher eigenvalues have similar asymptotic behavior, when the mesh is refined. (I shall not attempt to prove this, which is difficult,[6] but it can easily be checked for meshes with a regular, repetitive layout.) So we should compare the first positive eigenvalue $\lambda_1(\mathbf{M}_W)$ with its homologue $\lambda_1(\mathbf{M}_P)$. As we noticed, $\mathbf{M}_P$ is regular, in general. But zero is an eigenvalue of the curl–curl operator, and as a rule, spectral elements of an operator are approximated (when the mesh is repeatedly refined while

[6]The difficulty lies in *stating* the claim with both precision and generality.

keeping flatness under control, which we informally denote as "$m \to 0$") by those of its discrete matrix counterpart, which *does not contain* 0. *Therefore,* when $m \to 0$, $\lambda_1(\mathbf{M}_P)$ tends to 0. But for $\mathbf{M}_W$, the situation is quite different: This matrix is singular, since it contains the vectors $\mathbf{a} = \mathbf{G}\boldsymbol{\psi}$ (with $\boldsymbol{\psi}_n \neq 0$ for all n not in S^b). No need in consequence for the eigenvalue 0 to be approximated "from the right", as was the case for $\mathbf{M}_P$.

And indeed, $\lim_{m \to 0} \lambda_1(\mathbf{M}_W) > 0$. This can be seen by applying the Rayleigh quotients theory, according to which

$$\lambda_1(\mathbf{M}_W) = \inf\{(\mathbf{M}_W \mathbf{a}, \mathbf{a}) : |\mathbf{a}| = 1, (\mathbf{a}, \mathbf{a}') = 0 \ \forall \mathbf{a}' \in \ker(\mathbf{M}_W)\}.$$

In terms of the associated vector fields, this orthogonality condition means

$$\int_D \mathrm{a} \cdot \mathrm{grad}\, \psi' = 0 \quad \forall \psi' \in \Psi^0 \cap W^0_m, \tag{34}$$

where $\Psi^0 = \{\psi \in L^2_{\mathrm{grad}}(D) : \psi = 0 \text{ on } S^b\}$. Let $a_1(m)$ be the field whose DoFs form the eigenvector $\mathbf{a}_1$ corresponding to λ_1, and a_1 its limit when $m \to 0$. Equation (34) holds for a_1. Therefore (take the projections on W^0_m of ψ' in (34), and pass to the limit),

$$\int_D a_1 \cdot \mathrm{grad}\, \psi' = 0 \quad \forall \psi' \in \Psi^0,$$

and a_1 is thus divergence-free. Hence

$$\lim_{m \to 0} \lambda_1(\mathbf{M}_W) = \inf\{\int_D \sigma^{-1} |\,\mathrm{rot}\, a\,|^2 : a \in \tilde{A}^0, \ \mathrm{div}\, a = 0, \ \int_D |a|^2 = 1\},$$

and this Rayleigh quotient is strictly positive.

So we may conclude that $\kappa(\mathbf{M}_W)/\kappa(\mathbf{M}_P)$ tends to 0: Effective conditioning is asymptotically better with edge elements.

6.3.4 Yes, but ...

Is the case over? Not yet, because the defendants have still some arguments to voice. Ease in setting up boundary conditions? Yes, but think of all these standard finite element packages around. Reusing them will save much effort. Bad conditioning? Yes, but asymptotically so, and we don't go to the limit in practice; we make the best mesh we can, within limits imposed by computing resources; this mesh may not be the same for both methods, since the number of degrees of freedom will be different, so the comparison may well be of merely academic interest. Same thing about the relative loss of accuracy: Given the same resources, we may use more refined meshes in the case of nodal elements, since the number of degrees

of freedom is lower, apparently. After all, the number of edges E is much higher than 3N, isn't it?

Let us count again. Assume the mesh is first done with bricks, each of these being further divided into five tetrahedra (cf. Exer. 3.7). Thus, $T \approx 5N$. Then $F \approx 10\,N$ (four faces for each tetrahedron, shared by two), and the Euler–Poincaré formula, that is, as we know,

$$N - E + F - T = \chi(D),$$

shows that $E \approx 6N$. So indeed, the number of DoFs in the edge element method (about $E \approx 6N$) will be twice as high as in the nodal vectorial one ($\approx 3N$).

These figures, which ignore boundary conditions, are quite approximate (cf. [Ko] for precise counting). The ratios are valid for big meshes only. Still, the conclusion is neat: Tetrahedral edge elements generate more degrees of freedom than classical elements.

But is that really topical? The most meaningful number, from the point of view of data storage and CPU time, is not the size of the matrix, but the number of its nonzero entries. It happens this number is *smaller*, for a given mesh, for $\mathbf{M}_W$ than for $\mathbf{M}_P$, against pessimistic expectations.

For let us count the average number of entries on a given row of $\mathbf{M}_P$: This equals the number of DoFs that may interact with a given nodal one, that is, if we denote by v_i the basis vectors in a Cartesian frame, the number of couples $\{m, j\}$ for which $\int_D \mu^{-1}\,\mathrm{rot}\,(v_i w_n) \cdot \mathrm{rot}\,(v_j w_m) \neq 0$, for a given $\{n, i\}$. But $\mathrm{rot}\,(v_i w_n) = -\,v_i \times \mathrm{grad}\, w_n$, so this term vanishes if the supports of w_n and w_m don't intersect, so two DoFs may interact only when they belong to the same node, or to nodes linked by an edge. As each node is linked with about 12 neighbors, there are 38 extra-diagonal non-vanishing terms on a row of $\mathbf{M}_P$, on average.

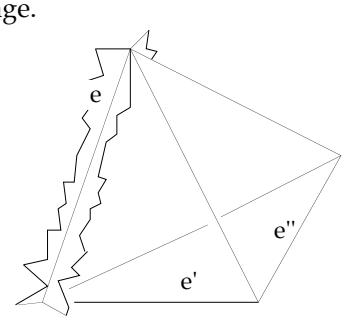

As for $\mathbf{M}_W$, the number of extra-diagonal non-vanishing terms on the row of edge e is the number of edges e' for which the integral $\int_D \mu^{-1}\,\mathrm{rot}\, w_e \cdot \mathrm{rot}\, w_{e'}$ differs from 0, that is, edges belonging to a tetrahedron that contains e. On the average, e belongs to 5 tetrahedra (because it belongs to 5 faces, since $F \approx 5E/3$, each face having 3 edges). This edge thus has 15 "neighbors" (inset): 10 edges which share a node with e, and 5 opposite in their common tetrahedron. So there are about 15

extra-diagonal nonzero entries per row, that is, about $90\,\mathrm{N}$ terms of this kind in $\mathbf{M}_W$, against $3 \times 38 = 114\,\mathrm{N}$ in $\mathbf{M}_P$, a sizable advantage in favor of edge elements.

This rather satisfying conclusion should not mask the obvious problem with *all* vector potential methods, whatever the finite elements: a large number of DoFs, relatively. In the same conditions as previously, the φ method only generates $12\mathrm{N}$ off-diagonal nonzero terms. In Appendix C, we shall see how some savings are possible, but only to some extent. Complementarity has its price.

6.3.5 Conclusion

Focusing on magnetostatics as I do in this book has obvious shortcomings, but also the advantage of delimiting a narrow field in which theory can deploy itself, and any fundamental observation in this limited area has all chances to be valid for magnetics in general. This seems to be the case of the nodal elements vs edge elements debate. But of course, theory will not carry the day alone, and numerical experience is essential. We have a lot of that already. It began with M. Barton's thesis [Br] (see an account in [BC]), whose conclusions deserve a quote:

> When the novel use of tangentially continuous edge-elements for the representation of magnetic vector potential was first undertaken, there was reason to believe it would result in an interesting new way of computing magnetostatic field distributions. There was only hope that it would result in a significant improvement in the state-of-the-art for such computations. As it has turned out, however, the new algorithm has significantly out-performed the classical technique in every test posed. The use of elements possessing only tangential continuity of the magnetic vector potential allows a great many more degrees of freedom to be employed for a given mesh as compared to the classical formulation; and these degrees of freedom result in a global coefficient matrix no larger than that obtained from the smaller number of degrees of freedom of the other method. (. . .) It has been demonstrated that the conjugate gradient method for solving sets of linear equations is well-defined and convergent for symmetric but underdetermined sets of equations such as those generated by the new algorithm. As predicted by this conclusion, the linear equations have been successfully solved for all test problems, and the new method has required significantly fewer iterations to converge in almost all cases than the classical algorithm.

One may also quote this [P&], about scattering computations:

> Experience with the 3D node-based code has been much more discouraging: many problems of moderate rank failed to converge within N iterations (. . .). The

Whitney elements were the only formulation displaying robust convergence with diagonal PBCG[7] iterative solution.

Countless objections have been raised against edge elements. The most potent one is that W^1, contrary to IP^1, does not contain globally linear vector fields, like for instance $x \rightarrow x$, and thus lack "first-order completeness". This is both true and irrelevant. In magnetostatics, where the object of attention is not the unknown a but its curl, we already disposed of the objection with Prop. 6.4. But even in eddy-current computations (where, as we'll see in Chapter 8, edge elements are natural approximants for the field h), it does no good to enlarge W^1 to the space spanned by the $w_n \nabla w_m$ (which does include linear fields). See [B4, DB, Mk].

The debate on this and other issues relative to the edge elements vs nodal elements contest winds its way and will probably go on for long, but it would be tedious to dwell on it. As one says, those who ignore history are bound to live it anew. A lot remains to be done, however: research on higher-order edge elements (to the extent that [Ne] does not close the subject), error analysis [Mk, MS, Ts], edge elements on other element forms than tetrahedra, such as prisms, pyramids, etc. [D&].

The problem of singularity addressed in Remark 6.4 is crucial, in practice, when there is a distributed source-term, as is the case in magnetostatics. If the discretization of the right-hand side is properly done, one will obtain a system of the form $\mathbf{R}^t\mathbf{M}_2(\sigma^{-1})\mathbf{R}\,\mathbf{a} = \mathbf{R}^t\mathbf{k}$, where $\mathbf{a}$ is the DoF-vector of the vector potential, and $\mathbf{k}$ a given vector, and in this case the right-hand side $\mathbf{R}^t\mathbf{k}$ is in the range of $\mathbf{R}^t\mathbf{M}_2(\sigma^{-1})\mathbf{R}$. But otherwise, the system has no solution, which the behavior of iterative algorithms tells vehemently (drift, as evoked in 6.3.3, slowed convergence, if not divergence). This seems to be the reason for the difficulties encountered by some, which can thus easily be avoided by making sure that the right-hand side behaves [Re]. There, again, tree–cotree techniques may come to the rescue.

Finally, let us brush very briefly on the issue of singularity. Should the edge-element formulation in a be "gauged", that is, should the process of selecting *independent* variables be pushed further, to the point of having only *non-redundant* DoFs? This can be done by extracting spanning trees. Such gauging is necessary with nodal elements, but not with edge elements. Experiments by Ren [Re] confirm this, which was already suggested by Barton's work.

[7]This refers to the "preconditioned biconjugate gradient" algorithm [Ja].

EXERCISES

See p. 171 for Exercise 6.1, p. 174 for Exer. 6.2, p. 179 for Exer. 6.3, and p. 174 for Exers. 6.4 and 6.5.

Exercise 6.6. Let a smooth surface S be equipped with a field of normals. Given a smooth function φ and a smooth vector field u, we may define the restriction of φ to S, or *trace* φ_S, the *tangential part* u_S of u (that is, the surface field of orthogonal projections of vector $u(x)$ onto the tangent plane at x, where x spans S, as in Fig. 2.5), and the *normal component* $n \cdot u$ of u. For smooth functions and tangential fields living on S, like φ_S and u_S, define operators grad_S, rot_S, and div_S in a sensible way, and examine their relationships, including integration-by-parts formulas.

HINTS

6.1. Notice that this approach amounts to solving (11) and (12′).

6.2. Their physical *dimension* is the key. Note that components of $\mathbf{L}\,\mathbf{a}$ are induction fluxes, and $(\mathbf{M}\,\mathbf{a}, \mathbf{a})$ has the dimension of energy.

6.3. For a tetrahedron T which contains $e = \{m, n\}$, integrate by parts the contribution $\int_T h \cdot \mathrm{rot}\, w_e$, hence a weighted sum of the jump $[n \times h]$ over ∂T. Check that faces opposite n or m contribute nothing to this integral. As for faces f which contain e, relate $\int_f [n \times h] \cdot w_e$ with the circulation of $[h]$ along the median. Use $\mathrm{rot}\, h_m = 0$ *inside* each tetrahedron to derive the conclusion.

6.4. Compute the divergence of $u = \sum_{n \in \mathcal{N}} \underline{\mathbf{u}}_n w_n$.

6.5. Take the curls.

6.6. Obviously, $\mathrm{grad}_S\, \varphi_S$ must be defined as $(\mathrm{grad}\, \varphi)_S$, and $\mathrm{rot}_S u_S$ as $n \cdot \mathrm{rot}\, u$, when φ and u live in 3D space, for consistency. (Work in x–y–z coordinates when S is the plane $z = 0$ to plainly see that.) Verify that these are indeed *surface* operators, that is, they only depend on the traces on S of fields they act on. Define div_S by Ostrogradskii–Gauss (in order to have a usable integration by parts formula on S), and observe its kinship with rot_S. You'll see that a second integration-by-parts formula is wanted. Use notation as suggested in inset.

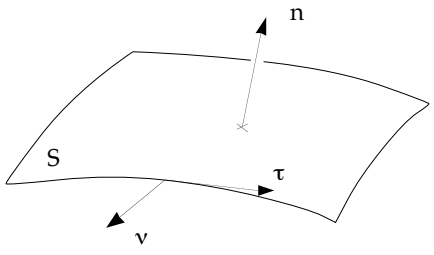

SOLUTIONS

6.1. It's equivalent to the two-stage optimization

$$\inf\{F \in \mathbb{R} : \ \inf\{h' \in \mathbb{H}^I,\ b' \in \mathbb{B}^F :\ E(b',\ h')\}\}$$

which indeed aims at the lowest error in constitutive law, given I.

6.2. Flux × mmf = energy, so all components of $\boldsymbol{\lambda}$ are magnetomotive forces. One of them is the driving mmf I applied between S^h_0 and S^h_1. All others are associated with faces which pave S^b, and assume the exact value necessary to cancel the induction flux through each of these faces.

6.3. Cf. Fig. 6.9.

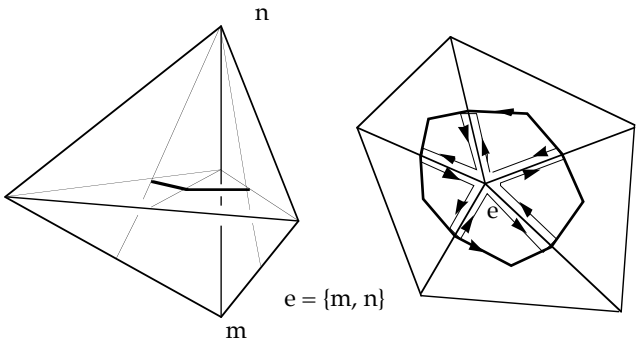

FIGURE 6.9. Same circulation of h along the equatorial circuit joining the barycenters of faces and volumes around e (i.e., the boundary of the dual cell e^*, cf. Fig. 4.4) and along the star-shaped circuit that radiates from edge e to the centers of faces containing e. The latter circulation is equal to $\int h \cdot \mathrm{rot}\, w_e$.

6.4. Elements of W^1 are divergence-free inside tetrahedra, whereas $\mathrm{div}\, u = \sum_{n \in \mathcal{N}} \underline{\mathbf{u}}_n \cdot \nabla w_n$ has no reason to vanish.

6.6. By Stokes, $n \cdot \mathrm{rot}\, u$ at point x is the limit $(\int_\gamma \tau \cdot u)/\mathrm{area}(\omega)$, where γ is the boundary of a shrinking surface domain ω enclosing x (see the inset in the "hints" section). Since $\tau \cdot u = \tau \cdot u_S$, only the tangential part u_S is involved. (Remark that only the orientation of γ matters here. The normal field serves to provide it, in association with the orientation of ambient space.) Note that $\nu = -n \times \tau$ is a surface field of outward unit normals with respect to ω. Since $\tau \cdot u_S = n \times \nu \cdot u_S = -\nu \cdot n \times u_S$, the circulation $\int_\gamma \tau \cdot u$ is also the outgoing flux (*along* the surface) of $-n \times u_S$, which suggests to define the surface divergence as

$$\mathrm{div}_S u_S = -\mathrm{rot}_S(n \times u), \tag{35}$$

also a surface operator by the same argument. The formula

$$\int_S u_S \cdot \mathrm{grad}_S \varphi_S = -\int_S \varphi_S \ \mathrm{div}_S u_S + \int_{\partial S} \varphi_S \nu \cdot u_S$$

(where ν now refers to the rim of S), is proved by the same technique as in dimension 3, but (35) suggests to also introduce a rot operator acting on *scalar* surface fields, as follows:

$$\mathrm{rot}_S \varphi_S = -n \times \mathrm{grad}_S \varphi_S,$$

hence the formula

$$\int_S \varphi_S \, \mathrm{rot}_S u_S = \int_S u_S \cdot \mathrm{rot}_S \varphi_S - \int_{\partial S} \varphi_S \tau \cdot u_S,$$

the nice symmetry of which compensates for the slight inconvenience[8] of overloading the symbol rot_S.

REFERENCES and Bibliographical Comments

The search for complementarity, a standing concern in computational electromagnetism [HP, HT], is related to the old "hypercircle" idea of Prager and Synge [Sy]. In very general terms, this method consisted in partitioning the set of equations and boundary conditions into two parts, thus defining two orthogonal subsets in the solution space, the solution being at their intersection. Finding two approximations within each of these subsets allowed one (by the equivalent of the Pythagoras theorem in the infinite dimensional solution space, as was done above in 6.3.1) to find the center and radius of a "hypercircle" containing the unknown solution, and hence the bounds (not only on quadratic quantities such as the reluctance, but on linear functionals and, even better, on pointwise quantities [Gr]). After a period of keen interest, the idea was partly forgotten, then revisited or rediscovered by several authors [DM, HP, LL, Ny, R&, Va, . . .], Noble in particular [No], who is credited for it by some (cf. Rall [Ra], or Arthurs [An], who also devoted a book to the subject [Ar]). Thanks to the Whitney elements technology, we may nowadays adopt a different (more symmetrical) partitioning of equations than the one performed by Synge on the Laplace problem. (The one exposed here was first proposed in [B1].) On pointwise estimates, which seem to stem from Friedrichs [Fr], see [Ba], [Co], [Ma], [St], [Sn].

[8]The risk of confusion, not to be lightly dismissed, will be alleviated by careful definition of the types of the fields involved: The first rot is *VECTOR* → *SCALAR* (fields), the other one is *SCALAR* → *VECTOR*. Various devices have been proposed to stress the distinction, including the opposition rot vs Rot, but they don't seem to make things more mnemonic. A. Di Carlo has proposed to denote the second operator by "grot", which would solve this terminological difficulty.

[A&] R. Albanese, R. Fresa, R. Martone, G. Rubinacci: "An Error Based Approach to the Solution of Full Maxwell Equations", **IEEE Trans., MAG-30**, 5 (1994), pp. 2969–2971.

[AE] P. Alfeld, D.J. Eyre: "The Exact Analysis of Sparse Rectangular Linear Systems", **ACM TOMS, 17,** 4 (1991), pp. 502–518.

[An] N. Anderson, A.M. Arthurs, P.D. Robinson: "Pairs of Complementary Variational Principles", **J. Inst. Math. & Applications, 5** (1969), pp. 422–431.

[Ar] A.M. Arthurs: **Complementary Variational Principles,** Clarendon Press (Oxford), 1970.

[Br] M.L. Barton: **Tangentially Continuous Vector Finite Elements for Non-linear 3-D Magnetic Field Problems**, Ph.D. Thesis, Carnegie-Mellon University (Pittsburgh), 1987.

[BC] M.L. Barton, Z.J. Cendes: "New vector finite elements for three dimensional magnetic fields computations", **J. Appl. Phys., 61**, 8 (1987), pp. 3919–3921.

[Ba] N.M. Basu: "On an application of the new methods of the calculus of variations to some problems in the theory of elasticity", **Phil. Mag., 7,** 10 (1930), pp. 886–896.

[B1] A. Bossavit: "Bilateral Bounds for Reluctance in Magnetostatics", in **Numerical Field Calculation in Electrical Engineering** (Proc. 3d Int. IGTE Symp.), IGTE (26 Kopernikusgasse, Graz, Austria), 1988, pp. 151–156.

[B2] A. Bossavit: "A Numerical Approach to Transient 3D Non-linear Eddy-current Problems", **Int. J. Applied Electromagnetics in Materials**, **1**, 1 (1990), pp. 65–75.

[B3] A. Bossavit: "Complementarity in Non-Linear Magnetostatics: Bilateral Bounds on the Flux-Current Characteristic", **COMPEL, 11**, 1 (1992), pp. 9–12.

[B4] A. Bossavit: "A new rationale for edge-elements", **Int. Compumag Society Newsletter, 1,** 3 (1995), pp. 3–6.

[Bw] K. Bowden: "On general physical systems theories", **Int. J. General Systems, 18** (1990), pp. 61–79.

[Co] Ph. Cooperman: "An extension of the method of Trefftz for finding local bounds on the solutions of boundary value problems, and on their derivatives", **Quart. Appl. Math., 10,** 4 (1953), pp. 359–373.

[DM] Ph. Destuynder, B. Métivet: "Estimation explicite de l'erreur pour une méthode d'éléments finis non conforme", **C.R. Acad. Sci. Paris, Série I** (1996), pp. 1081–1086.

[DB] D.C. Dibben, R. Metaxas: "A Comparison of the Errors Obtained with Whitney and Linear Edge Elements", **IEEE Trans., MAG-33**, 2 (1997), pp. 1524–1527.

[D&] P. Dular, J.-Y. Hody, A. Nicolet, A. Genon, W. Legros: "Mixed Finite Elements Associated with a Collection of Tetrahedra, Hexahedra and Prisms", **IEEE Trans., MAG-30**, 5 (1994), pp. 2980–2983.

[Fe] W. Fenchel: "On Conjugate Convex Functions", **Canadian J. Math., 1** (1949), pp. 23–27.

[Fr] R.L. Ferrari: "Complementary variational formulations for eddy-current problems using the field variables E and H directly", **IEE Proc**., **Pt. A**, **132**, 4 (1985), pp. 157–164.

[Fr] K.O. Friedrichs: "Ein Verfahren der Variationsrechnung, das Minimum eines Integrals als das Maximum eines Anderen Ausdruckes darzustellen", **Nachrichten der Ges. d. Wiss. zu Göttingen** (1929), p. 212.

[Gr] H.J. Greenberg: "The determination of upper and lower bounds for the solution of the Dirichlet problem", **J. Math. Phys., 27** (1948), pp. 161–182.

[HP] P. Hammond, J. Penman: "Calculation of inductance and capacitance by means of dual energy principles", **Proc. IEE, 123**, 6 (1976), pp. 554–559.

[HT] P. Hammond, T.D. Tsiboukis: "Dual finite-elements calculations for static electric and magnetic fields", **IEE Proc., 130, Pt. A,** 3 (1983), pp. 105–111.

[Ja] D.A.H. Jacobs: "Generalization of the Conjugate Gradient Method for Solving Non-symmetric and Complex Systems of Algebraic Equations", CEGB Report RD/L/N70/80 (1980).

[Ke] L. Kettunen, K. Forsman, D. Levine, W. Gropp: "Volume integral equations in nonlinear 3-D magnetostatics", **Int. J. Numer. Meth. Engng., 38** (1995), pp. 2655–2675.

[Ko] P.R. Kotiuga: "Analysis of finite-element matrices arising from discretizations of helicity functionals", **J. Appl. Phys., 67**, 9 (1990), pp. 5815–5817.

[LL] P. Ladévèze, D. Leguillon: "Error estimate procedure in the finite element method and applications", **SIAM J. Numer. Anal., 20,** 3 (1983), pp. 485–509.

[Ma] C.G. Maple: "The Dirichlet problem: Bounds at a point for the solution and its derivative", **Quart. Appl. Math., 8,** 3 (1950), pp. 213–228.

[Mk] P. Monk: "A finite element method for approximating the time-harmonic Maxwell equations", **Numer. Math., 63** (1992), pp. 243–261.

[MS] P. Monk, E. Süli: "A convergence analysis of Yee's scheme on nonuniform grids", **SIAM J. Numer. Anal., 31**, 2 (1994), pp. 393–412.

[Mo] J.J. Moreau: **Fonctionnelles convexes**, Séminaire Leray, Collège de France, Paris (1966).

[Ny] B. Nayroles: "Quelques applications variationnelles de la théorie des fonctions duales à la mécanique des solides", **J. de Mécanique, 10**, 2 (1971), pp. 263–289.

[Ne] J.C. Nedelec: "A new family of mixed finite elements in $\mathbb{R}^3$ ", **Numer. Math., 50** (1986), pp. 57–81.

[No] B. Noble: "Complementary variational principles for boundary value problems I: Basic principles with an application to ordinary differential equations", MRC Technical Summary Report N° 473, Nov. 1964.

[OR] J.T. Oden, J.N. Reddy: "On Dual Complementary Variational Principles in Mathematical Physics", **Int. J. Engng. Sci., 12** (1974), pp. 1–29.

[P&] J. Parker, R.D. Ferraro, P.C. Liewer: "Comparing 3D Finite Element Formulations Modeling Scattering from a Conducting Sphere", **IEEE Trans., MAG-29**, 2 (1993), pp. 1646–1649.

[PF] J. Penman, J.R. Fraser: "Dual and Complementary Energy Methods in Electro-magnetism", **IEEE Trans., MAG-19**, 6 (1983), pp. 2311–2316.

[PT] Y. Perréal, P. Trouvé: "Les méthodes variationnelles pour l'analyse et l'approximation des équations de la physique mathématique: Les méthodes mixtes-hybrides conservatives", **Revue Technique Thomson-CSF, 23**, 2 (1991), pp. 391–468.

[Ra] L.B. Rall: "On Complementary Variational Principles", **J. Math. Anal. & Appl., 14** (1966), pp. 174–184.

[Re] Z. Ren, in A. Bossavit, P. Chaussecourte (eds.): **The TEAM Workshop in Aix-les-Bains,** July 7–8 1994, EdF, Dpt MMN (1 Av. Gal de Gaulle, 92141 Clamart), 1994.

[R§] J. Rikabi, C.F. Bryant, E.M. Freeman: "An Error-Based Approach to Complementary Formulations of Static Field Solutions", **Int. J. Numer. Meth. Engnrg., 26** (1988), pp. 1963–1987.

[Ro] R.T. Rockafellar: **Convex Analysis**, Princeton U.P. (Princeton), 1970.

[Rt] J.P. Roth: "An application of algebraic topology: Kron's method of tearing", **Quart. Appl. Math., 17,** 1 (1959), pp. 1–24.

[St] H. Stumpf: "Über punktweise Eingrenzung in der Elastizitätstheorie. I", **Bull. Acad. Polonaise Sc., Sér. Sc. Techniques, 16,** 7 (1968), pp. 329–344, 569–584.

[Sn] J.L. Synge: "Pointwise bounds for the solutions of certain boundary-value problems", **Proc. Roy. Soc. London, A 208** (1951), pp. 170–175.

[Sy] J.L. Synge: **The Hypercircle in Mathematical Physics,** Cambridge University Press (Cambridge, UK), 1957.

[To] E. Tonti: "On the mathematical structure of a large class of physical theories", **Lincei, Rend. Sc. fis. mat. e nat., 52,** 1 (1972), pp. 51–56.

[Ts] I.A. Tsukerman: "Node and Edge Element Approximation of Discontinuous Fields and Potentials", **IEEE Trans., MAG-29,** 6 (1993), pp. 2368–2370.

[Va] M.N. Vaïnberg: **Variational Methods for the Study of Nonlinear Operator Equations,** Holden Day (San Francisco), 1963. (Russian edition: Moscow, 1956.)